BBA - Molecular Basis of Disease 1865 (2019) 774–781

Contents lists available at ScienceDirect

BBA - Molecular Basis of Disease

journal homepage: www.elsevier.com/locate/bbadis

Sphingosine-1-phosphate promotes barrier-stabilizing effects in human microvascular endothelial cells *via* AMPK-dependent mechanisms☆

Sophie Dennhardt[a,b,c,1], Karl R. Finke[a,b,1], Andrea Huwiler[d], Sina M. Coldewey[a,b,c,*]

[a] Department of Anaesthesiology and Intensive Care Medicine, Jena University Hospital, Jena, Germany
[b] Septomics Research Centre, Jena University Hospital, Jena, Germany
[c] Center for Sepsis Control and Care, Jena University Hospital, Jena, Germany
[d] Institute of Pharmacology, University of Bern, Inselspital, Bern, Switzerland

ARTICLE INFO

Keywords:
AMP-dependent kinase
Sphingosine-1-phosphate
Endothelial barrier
Barrier breakdown
Inflammation
ECIS

ABSTRACT

Breakdown of the endothelial barrier is a critical step in the development of organ failure in severe inflammatory conditions such as sepsis. Endothelial cells from different tissues show phenotypic variations which are often neglected in endothelial research. Sphingosine-1-phosphate (S1P) and AMP-dependent kinase (AMPK) have been shown to protect the endothelium and phosphorylation of AMPK by S1P was shown in several cell types. However, the role of the S1P-AMPK interrelationship for endothelial barrier stabilization has not been investigated. To assess the role of the S1P-AMPK signalling axis in this context, we established an *in vitro* model allowing real-time monitoring of endothelial barrier function in human microvascular endothelial cells (HMEC-1) and murine glomerular endothelial cells (GENCs) with the electric cell-substrate impedance sensing (ECIS™) system. Following the disruption of the cell barrier by co-administration of LPS, TNF-α, IL-1ß, IFN-γ, and IL–6, we demonstrated self-recovery of the disrupted barrier in HMEC-1, while the barrier remained compromised in GENCs. Under physiological conditions we observed a rapid phosphorylation of AMPK in HMEC-1 stimulated with S1P, but not in GENCs. Consistently, S1P enhanced the basal endothelial barrier in HMEC-1 exclusively. siRNA-mediated knockdown of AMPK in HMEC-1 led to a less pronounced barrier enhancement. Thus we present evidence for a functional role of AMPK in S1P-mediated barrier stabilization in HMEC-1 and we provide insight into cell-type specific differences of the S1P-AMPK-interrelationship, which might influence the development of interventional strategies targeting endothelial barrier dysfunction.

1. Introduction

Systemic inflammation in the critically ill patient is often accompanied by an impairment of the microcirculation [1] that contributes to the development of organ dysfunction [2]. The exposure of the microvascular endothelium to inflammatory mediators can result in an activated pro-coagulant state with microthrombi formation as well as a severe impairment of the endothelial barrier [3]. This leads to capillary leakage and interstitial oedema resulting in decreased tissue oxygenation facilitating the onset of organ dysfunction [4]. Thus, the development of preventive or therapeutic strategies stabilizing endothelial barriers may improve the outcome in patients suffering from conditions associated with severe systemic inflammation, such as sepsis.

Sphingosine-1-phosphate (S1P) is a bioactive lipid mediator circulating mostly in the blood, influencing cellular migration, proliferation and survival *via* its G protein-coupled receptors $S1P_{1–5}$ [5]. S1P potently promotes barrier function *in vitro* [6–8] and is essential for maintenance of endothelial barriers *in vivo* [9,10]. Our group and others have shown that serum S1P levels are lower in septic patients and correlate negatively with the severity of disease. This indicates a role of S1P in the pathophysiology of endothelial dysfunction [11–13]. FTY720 – a clinically approved S1P analogue for treatment of multiple sclerosis – enhances the endothelial barrier in cultured pulmonary or brain endothelial cells [14–16] and reduces barrier-permeabilizing effects of

Abbreviations: AMPK, AMP-dependent kinase; ECIS, electric cell-substrate impedance sensing; GENCs, glomerular endothelial cells; HMEC-1, human microvascular endothelial cells; S1P, sphingosine-1-phosphate

☆ This article is part of a Special Issue entitled: The power of metabolism: Linking energy supply and demand to contractile function edited by Torsten Doenst, Michael Schwarzer and Christine Des Rosiers.

* Corresponding author at: Department of Anaesthesiology and Intensive Care Medicine, Jena University Hospital, Am Klinikum 1, 07747 Jena, Germany.
E-mail address: sina.coldewey@med.uni-jena.de (S.M. Coldewey).

[1] SD and KRF contributed equally.

https://doi.org/10.1016/j.bbadis.2018.12.022
Received 8 August 2018; Received in revised form 20 December 2018; Accepted 21 December 2018
Available online 17 January 2019

VEGF [17] and TNF–α [15,18]. In a previous study by our group, administration of FTY720 improved cardiac dysfunction and was associated with elevated S1P serum levels in murine sepsis models [11]. Others have further shown that FTY720 reduces fluid extravasation in a rat model of sepsis [19] and lung microvascular permeability in LPS-challenged mice [20]. Additionally, Imeri et al. [15,18] reported a protective effect of FTY720 and S1P in the human endothelial cell line EA.hy 926 and in mouse and human microcapillary brain endothelial cells. This protection was suggested to involve an upregulation of the adherens junction molecule PECAM-1 (CD31) [15]. Targeting the S1P pathway might consequently be an interesting therapeutic approach to stabilize microvascular endothelial barriers. The effects of FTY720 on the glomerular endothelium in an inflammatory state have not yet been investigated.

The heterotrimeric AMP-dependent protein kinase (AMPK) is widely expressed in the endothelium [21] and previous *in vivo* and *in vitro* studies have shown that AMPK exerts anti-inflammatory and protective effects on the endothelial barrier under inflammatory conditions [22–24]. Of note, S1P is one of the agonists that can activate AMPK and targets further downstream in cultured bovine aortic cells [25] as well as human umbilical vein endothelial cells and baby hamster kidney cells [26,27] indicating that AMPK could be one of the mediators promoting the barrier-enhancing effects of S1P. However, the interaction of S1P and AMPK has not yet been investigated in the microvascular endothelium and the functional relevance of their interrelationship for the endothelial barrier remains unclear.

Although barrier dysfunction mainly affects the microvasculature, cells derived from the macrovasculature are often used to study endothelial barrier breakdown. It has previously been shown that endothelial cells have heterogeneous phenotypes regarding their permeability depending on the vascular branch from which they originate. This is, at least in part, influenced by different patterns of adhesion molecule and tight junction expression [28]. Tissue of origin also plays an important role, *e.g.* glomerular endothelium is highly fenestrated whereas both brain and dermal microvascular endothelial cells belong to the continuous endothelium. Still, brain and dermal microvascular endothelial cells differ regarding their caveolin as well as tight junction protein expression [28]. However, this fact is often neglected and might explain why *in vitro* observations often deviate from *in vivo* findings [29].

In this study we aimed to establish an *in vitro* model of inflammatory barrier breakdown in the microcirculation that is applicable to endothelial cell lines of various origins (species and tissue) in the electric cell-substrate impedance sensing (ECIS™) system. In addition to human microvascular endothelial cells (HMEC-1), we employed murine glomerular endothelial cells (GENCs), as the kidney is very sensitive to inflammation-induced organ failure [30] and the glomerular endothelium plays a key role in the progression of renal dysfunction [31]. S1P can phosphorylate AMPK in cells of the human [26] and bovine [25] macrovasculature as well as in kidney fibroblasts [27]. However, data on the S1P-AMPK interrelation in the microvasculature have not been reported. Therefore, we investigated the time courses of AMPK phosphorylation by S1P in HMEC-1 and GENCs. Subsequently, we evaluated the physiological relevance of this phosphorylation by siRNA-mediated knockdown of AMPK α1/2 in HMEC-1, which was implemented in the ECIS™ system by a reverse transfection protocol. Finally, we assessed effects of FTY720 on inflammatory barrier breakdown in HMEC-1 and GENCs using the *in vitro* model established in this study.

2. Methods

2.1. Cell culture

Cell culture media and supplements were purchased by Gibco unless stated otherwise. HMEC-1 were obtained from Centers for Disease Control and Prevention (CDC, Atlanta, reference number E-036-91/0) and cultured in MCDB131 medium supplemented with 10% fetal bovine serum (FBS), 1% glutamine, 10 ng/ml epidermal growth factor and 1 μg/ml hydrocortisone as well as 1% penicillin/streptomycin. HMEC-1 were passaged at 70–80% confluence and used from passage 4–15. GENCs isolated from immorto mice were obtained from Michael P. Madaio [32]. Cells were cultured in a DMEM low glucose, pyruvate medium with 23% Ham's F12 Nutrient Mix, 1% penicillin/streptomycin (Millipore) with 10% heat-inactivated FBS. GENCs were passaged at 60–70% confluence and cells from passages 5–9 were used in the experiments.

2.2. Inflammatory stimulus

Inflammatory conditions were simulated using an inflammatory stimulus (LPS + Cyt) containing the endotoxin lipopolysaccharide (LPS, 100 ng/ml, see Suppl. Table 1) and the pro-inflammatory cytokines TNF-α (100 μg/ml), IL-1ß (10 μg/ml), IFN-γ (10 μg/ml) and IL–6 (10 μg/ml). Stock solutions were prepared in DMEM with 1% bovine serum albumin (BSA, Sigma Aldrich) and were used at dilutions of 1:100, 1:400 and 1:1000 for GENCs. Stock solutions for HMEC-1 cells were prepared in MCDB131 with 1% BSA and used at dilutions of 1:100, 1:400 and 1:800.

2.3. Measuring endothelial barrier function

Endothelial barrier function was evaluated using the ECIS™ Zθ system (Applied Biophysics) [33]. 8W10E ECIS Cultureware™ Arrays (Applied Biophysics) were coated with a solution containing fibronectin from human plasma (1 mg/ml, Biochrome) and mouse collagen IV (640 μg/ml, BD Biosciences) in phosphate-buffered saline (PBS). Electrodes were stabilized *via* the ECIS™ software. Measurements were performed in MFT (multiple frequencies per time) mode. Cells were seeded at a density of 10,000 cells/well (GENCs) or 20,000 cells/well (HMEC-1). Partial media changes were performed every 24 h until plateaus in both resistance (around 1200–1400 Ω in GENCs, around 1500–1800 Ω in HMEC-1) and confluence (around 5 nF for both cell lines) were reached. Once plateau was observed (approx. 72 h after seeding the cells), 200 μl medium were replaced with fresh medium containing inflammatory stimulus in various concentrations. S1P was added at 1 μM without change of medium. Resistance was monitored at 4000 Hz and capacitance at 64,000 Hz. Each manipulation was performed in duplicates. Time was resampled to 600 s and medium control was subtracted from the mean value of each measurement for normalization.

2.4. Cell stimulation with S1P

48 h prior to stimulation, cells were seeded in 35 mm culture dishes at a density of 50,000 cells/dish (GENCs) or 100,000 cells/dish (HMEC-1). Cells were subjected to serum starvation 4 h prior to the experiments. Cells were stimulated with 1 μM S1P (Sigma Aldrich, solubilized in methanol) or the same amount of vehicle for indicated times at 37 °C. In each experiment, stimulation with 2 mM AICAR (aminoimidazole carboxamide ribonucleotide, CST, solubilized in water) for 30 min served as a positive control for AMPK phosphorylation. Cells were washed, lysed on ice with lysis buffer (1% IGEPAL® CA-630, 50 mM Tris pH 8.0, 150 mM NaCl, 5 mM NaF, 1 mM Na_3VO_4, protease inhibitor cocktail 1:100) and centrifuged at 4 °C and 900 RCF for 7 min. Protein concentration was determined using Pierce Detergent Compatible Bradford Assay Kit (Thermo Fisher Scientific) according to the manufacturer's protocol and samples were processed with 4× SDS sample buffer (50 mM Tris pH 6.8, 2% SDS, 10% glycerol, 1% β-mercaptoethanol, 12.5 mM EDTA, 0.02% bromophenol blue) for immunoblotting.

2.5. Immunoblotting

20 µg of protein were loaded onto 10% TGX Stain-Free™ FastCast™ gels (Bio-Rad). Protein was transferred onto low fluorescent PVDF membranes (Bio-Rad) using the Trans-Blot® Turbo RTA Transfer Kit and Trans-Blot® Turbo™ Transfer system (Bio-Rad). Membranes were blocked in 5% BSA. AMPK α1/2 (CST, LOT no. 19), AMPK α1/2 pThr^{172} (CST, LOT no. 15) and β-actin (CST, LOT no. 13) antibodies were used at concentrations of 1:1000. Anti-rabbit IgG, HRP-linked secondary antibody (CST, LOT no. 27) and anti-mouse IgG, HRP-linked secondary antibody (CST, LOT no. 33) were used at a concentration of 1:2000. For signal detection, Clarity™ Western ECL substrate (Bio-Rad) and the ChemiDoc™ MP Imaging System (Bio-Rad) were used. First, the phospho-signal was detected, then membranes were stripped 15 min at 50 °C (stripping buffer: 20% SDS, 6.25 mM Tris pH 6.8, 0.8% β-mercaptoethanol) and reprobed with the AMPK α1/2 antibody. Signals were analysed and background was subtracted using the Image Lab™ software (Bio-Rad). Phosphorylation levels of AMPK were calculated by dividing AMPK phospho-Thr^{172} level by total AMPK α1/2 level (Σ AMPK α1/2). The ratio was normalized to the ratio of the respective unstimulated control. For analysis of knockdown efficiency, AMPK α1/2 level was normalized to β-actin and the percentage of remaining AMPK α1/2 signal was calculated relatively to the respective scrambled siRNA control band. Additionally, knockdown efficiency was calculated by Stain-Free™ quantification (Supplementary material).

2.6. Reverse transfection

The concept of reverse transfection of plasmids was introduced in 2001 by Ziauddin and Sabatini [34] and already successfully applied to siRNA transfection in the ECIS™ system [35]. For reverse transfection, cells were directly mixed with the transfection reagent instead of seeding them prior to the transfection protocol. This allowed performing the transfection process without complete media changes that are difficult to conduct in the ECIS™ system and avoided the need to split transfected cells before monitoring them. Control siRNA (scrambled siRNA), AMPK α1/2 siRNA as well as siRNA Transfection Reagent were purchased by Santa Cruz Biotechnology. The manufacturer's protocol was adapted to the smaller volumes used in ECIS™ arrays (400 µl instead of 1 ml) and optimal siRNA as well as Transfection Reagent dilution which was assessed in 6-well plates. For reverse transfection in the ECIS™ system, 1.6 µl siRNA as well as 1.6 µl Transfection Reagent per well were prepared according to the adapted protocol, incubated 45 min at RT, pipetted into the respective wells and mixed with 1×10^5 cells. ECIS™ measurement was started immediately thereafter. 5 h later, FBS and antibiotics were added to a final concentration of 10% and 1%, respectively. To remove transfection medium after 24 h, wash-out was performed by 5 partial changes. Medium was partially changed again after 48 h. After 72 h, S1P stimulation was performed by adding S1P directly to each well to a final concentration of 1 µM. Time was resampled to 600 s, medium control was subtracted from each measurement for normalization, and changes were calculated relative to 10 min before S1P stimulation.

2.7. FTY720 co-stimulation

Cells were seeded to the ECIS™ array and cultivated until resistance and capacitance plateaued as described above (Section 2.3). Subsequently, 200 µl medium were replaced with fresh medium containing either only inflammatory stimulus, the stimulus and FTY720 (LPS + Cyt 1:400 for HMEC-1 and 1:1000 for GENCs; FTY720 from Cayman Chemical solubilized in DMSO and added at 1 µM) or inflammatory stimulus and DMSO as vehicle.

2.8. Statistical analysis

Statistical analysis was performed using GraphPad Prism 7.03 software. Data are depicted as mean + SD for *n* number of independent experiments. For ECIS™ curves, normalized mean values and standard deviation were plotted against time starting from the stimulation. Statistics were performed as two-way ANOVA with Holm-Sidak *post hoc* test. Non-parametrical data was analysed by Mann-Whitney-*U* test. Outliers were excluded using ROUT test with $Q = 5$.

3. Results and discussion

3.1. Endothelial response to inflammatory conditions differs in HMEC-1 and GENCs

To establish an *in vitro* model of inflammatory barrier breakdown, confluent layers of two different cell lines were challenged with LPS + Cyt to mimic an inflammatory environment rather than studying isolated effects of one inflammatory agent. Changes in resistance were monitored with the ECIS™ system for a period of 24 h.

HMEC-1 responded to the inflammatory stimulus with an initial increase in resistance that was significant only in the lowest concentration tested (Fig. 1A). After approximately 2 h, resistance significantly decreased compared with the control reaching a minimum peak at around 6 h. This phase of decreased resistance resembling barrier dysfunction was shortest in the lowest concentration tested and most pronounced with LPS + Cyt 1:400. The endothelial barrier function of HMEC-1 subsequently recovered and reached a plateau that was significantly higher in LPS + Cyt 1:100 than in the respective control.

GENCs initially responded with a slight, non-significant increase in resistance (Fig. 1B). After that, resistance slightly decreased under the level of the control starting with LPS + Cyt 1:100 approximately 4 h, LPS + Cyt 1:400 approximately 5 h and last, LPS + Cyt 1:1000 approximately 7 h after stimulation. Until the end of the experiment, all curves with LPS + Cyt remained significantly lower than the control. Medium rescue was performed to test whether LPS + Cyt induced permanent damage to the endothelial layer of GENCs (Fig. 1C). After medium was changed, resistance rapidly recovered to levels that were comparable to the untreated control.

Cytoskeletal filaments are known for their important role in barrier stabilization [36] and LPS was shown to contribute to the disorganization of such filaments resulting in the formation of intracellular gaps in different endothelial cell lines [37,38]. As the changes in HMEC-1 barrier function were linked to significant changes in the confluence of the cell layer (Suppl. Fig. 1A), but occurred fast and were completely reversible, they are most probably caused by such fast reorganization processes in the cytoskeleton resulting in disturbances of cell-cell-contacts. The initial response of GENCs was comparable with HMEC-1 but less pronounced. Decrease in resistance and hereby endothelial barrier breakdown started considerably later and in contrast to HMEC-1, no recovery was observed in this cell line even after 24 h. Of note, capacitance also gradually and significantly increased with the decrease in barrier function (Suppl. Fig. 1B), indicating either cell death or pronounced changes in the cytoskeleton.

In conclusion, the inflammatory stimulus induced endothelial barrier dysfunction in HMEC-1 and GENCs, indicated by a significant decrease of resistance. However, the time course and the capability to recover from the LPS + Cyt challenge significantly differed in the two cell lines. In GENCs, a proportional change of medium allowed the endothelial barrier to recover rapidly. This indicates that the model is suitable to study barrier-recovering interventional strategies.

3.2. AMPK is phosphorylated upon S1P stimulation in HMEC-1 but not GENCs

Prior to testing interventional strategies in the established barrier

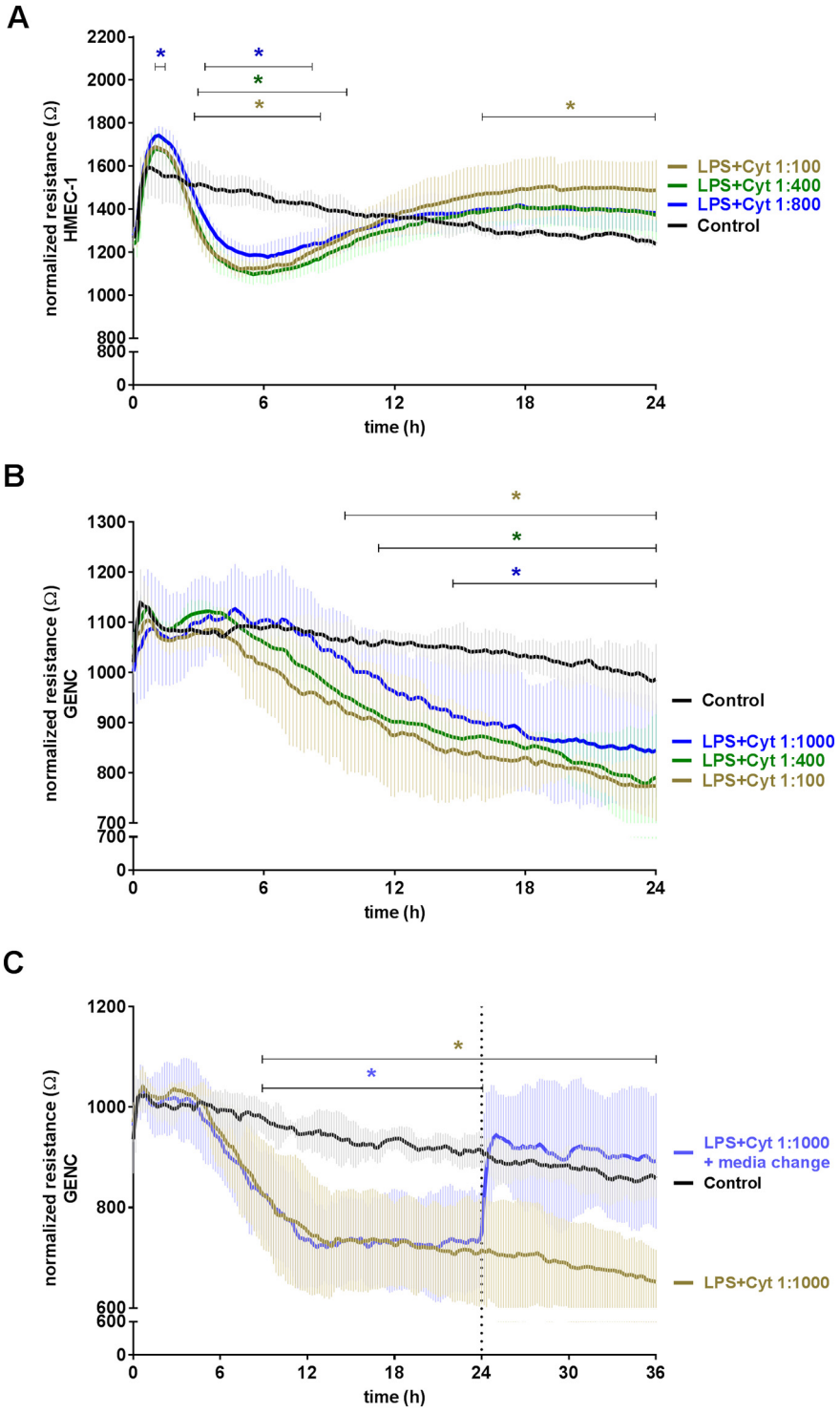

Fig. 1. Endothelial response to inflammatory conditions differs in HMEC-1 and GENCs. ECIS measurement of endothelial barrier function in (A) HMEC-1 (n = 3) and (B) GENCs (n = 3–4) stimulated with LPS, TNF-α, IL-1ß, IFN-γ, and IL–6 (LPS + Cyt) in the respective concentrations 72 h after cell seeding (t = 0 h). (C) Medium rescue performed by partial media change (indicated by vertical line) 24 h after stimulation with LPS + Cyt (t = 0 h) in GENCs (n = 3). (A–C) Data are expressed as mean ± SD, n = 3–4 measurements, *p < 0.05 *vs.* control at each respective time point is indicated by bars (two-way ANOVA with Holm-Sidak *post hoc*).

breakdown model, we aimed to characterize the interrelation of S1P and AMPK in each cell line under basal conditions. AMPK phosphorylation upon stimulation with S1P has been reported [25–27], but not yet assessed in cells of the microvasculature. We stimulated HMEC-1 and GENCs with 1 μM S1P for different time periods to investigate the course of AMPK phosphorylation. In HMECs, AMPK α1/2 was rapidly phosphorylated at Thr172 upon S1P stimulation (Fig. 2A, B). Considerably higher levels of phosphorylation were observable 1 min and 2 min after onset of stimulation compared with unstimulated control, which thereafter, decreased over time to levels that are comparable with unstimulated cells. This phosphorylation pattern was absent in the vehicle control performed in parallel (Suppl. Fig. 2A). S1P stimulation of confluent HMEC-1 cells led to a significant increase in resistance and hereby barrier function 2–5 h after onset of stimulation

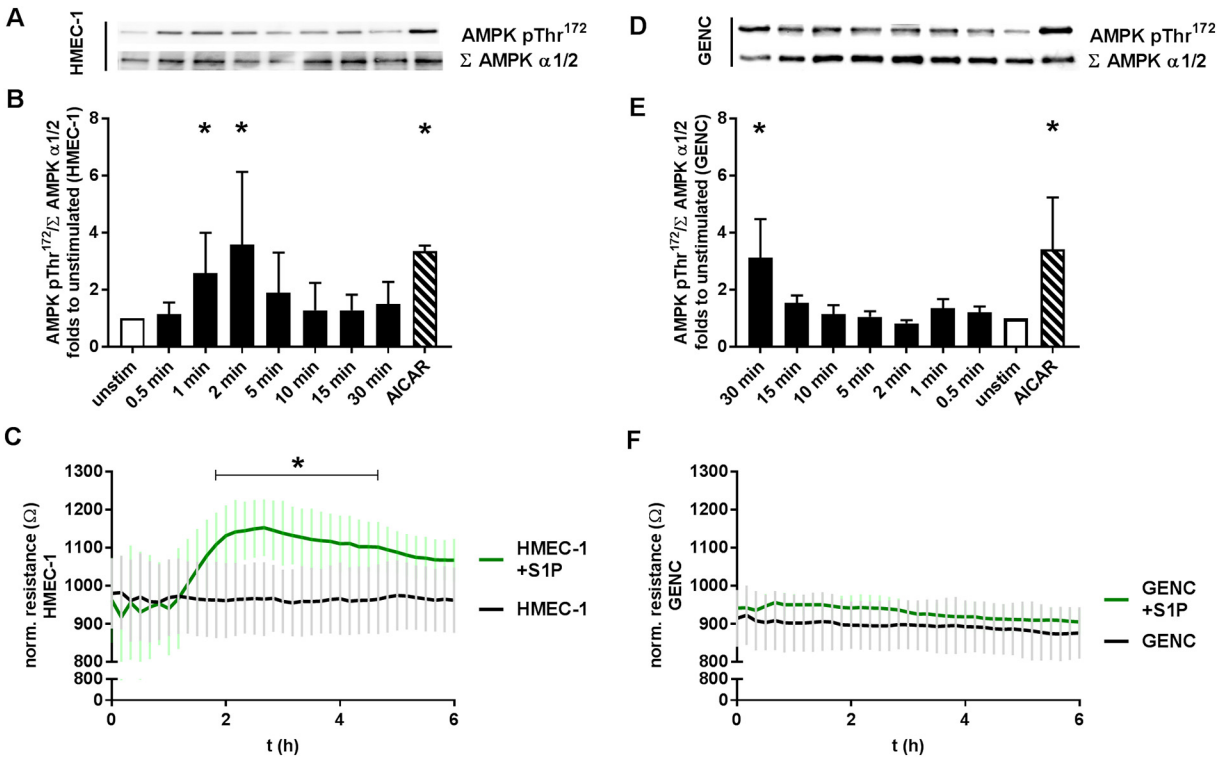

Fig. 2. S1P induces AMPK phosphorylation at Thr172 and increases barrier function in HMEC-1 but not in GENC. (A) Representative Western blots of HMEC-1 and (B) corresponding semi-quantification data expressed as mean + SD of 4 experiments. *p < 0.05 *vs.* unstimulated (Mann-Whitney-*U* test). (C) ECIS measurement of HMEC-1 (n = 9 measurements in 3 independent experiments) stimulated with 1 μM S1P 72 h after cells were seeded (t = 0). Data are expressed as mean ± SD. *p < 0.05 *vs.* HMEC-1 at each respective time point indicated by bars (two-way ANOVA with Holm-Sidak *post hoc*). (D) Representative Western blots of GENC and (E) corresponding semi-quantification data expressed as mean + SD of 4 experiments. *p < 0.05 *vs.* unstimulated (Mann-Whitney-*U* test). (F) ECIS measurement of GENC (n = 3) stimulated with 1 μM S1P 72 h after cells were seeded (t = 0). Data are expressed as mean ± SD (two-way ANOVA with Holm-Sidak *post hoc*).

(Fig. 2C). In GENCs, no significant changes in AMPK phosphorylation were detected in the period of observation except for 30 min of stimulation (Fig. 2D, E). However, the same effect was observed in the vehicle control (Suppl. Fig. 2B). In GENCs, we did not observe significant effects of S1P on endothelial barrier, consistent with absent AMPK phosphorylation (Fig. 2F).

S1P induced the phosphorylation of AMPK and enhanced the endothelial barrier in HMEC-1, a cell line shown to express the $S1P_1$ receptor [39,40]. As S1P had no effect on AMPK and endothelial barrier in GENCs this raised the question whether the cell line expresses the $S1P_1$ receptor. To address this question, we performed flow cytometry analysis to examine surface expression of $S1P_1$ in GENCs (Suppl. Material). The receptor was expressed in this cell line (Suppl. Fig. 3). A possible explanation for the differences in HMEC-1 and GENCs might be differential expression of $S1P_2$, a receptor partially antagonizing the effects of $S1P_1$ [41]. The balance between the two receptors influences S1P action on endothelial permeability [41]. It was shown *in vivo* that S1P was unable to prevent barrier breakdown in rat cremaster muscle vasculature unless $S1P_2$-signalling was inhibited by a selective inhibitor [42]. Taken together, since S1P in the used dosage did not induce phosphorylation of AMPK in GENCs and did not alter barrier function despite the presence of $S1P_1$, we hypothesize that this pathway is less relevant for barrier enhancement in the glomerular endothelium of mice. However, further studies should address the role of the different S1P receptors in the S1P-AMPK-interrelationship.

3.3. AMPK partially mediates the barrier-stabilizing effects of S1P in HMEC-1

Barrier protection mediated by either S1P [6–8] or AMPK activation [22–24] was reported in a variety of endothelial cell lines and we were able to demonstrate AMPK phosphorylation as well as an increase in endothelial barrier function upon S1P stimulation in HMEC-1. Therefore, the question arises whether S1P-mediated AMPK phosphorylation also contributes to the stabilization of endothelial barriers. To further examine this hypothesis, we established a reverse transfection protocol to knock down AMPK α1/2 in HMEC-1. AMPK was knocked down partially with 44% ± 11% of AMPK α1/2 remaining as determined by immunoblot analysis (Fig. 3A). When using Stain-Free™ in comparison to β-actin loading control for quantification, the knockdown efficiency was similar with 43% ± 9% of AMPK α1/2 remaining (Suppl. Fig. 4). Of note, cells with AMPK knockdown did not exhibit a different phenotype compared to cells treated with scrambled siRNA before cells were stimulated with S1P. In AMPK-deficient cells, stimulation with 1 μM S1P induced a rapid short-term decrease in resistance followed by an increase that was slightly lower than in cells treated with scrambled siRNA (Fig. 3B). Overall, the profile of endothelial resistance was similar. However, mean changes in resistance were significantly lower in AMPK-deficient cells compared with cells treated with scrambled siRNA ($p = 0.0059$, Fig. 3C).

Our observation that the endothelial barrier is not compromised in AMPK-deficient microvascular endothelial cells under basal conditions is in line with the study by Creighton et al. demonstrating that AMPK contributes to the development of endothelial barriers but not to their maintenance [43]. This as well as the achieved proportion of the AMPK knockdown of 44 ± 11% remaining AMPK α1/2 might explain the relatively small effect of S1P stimulation after AMPK knockdown observed in our study. Although the effect is small, the change in resistance in response to S1P was observed reproducibly in every replicate experiment performed indicating that AMPK could be involved in the regulation of S1P-mediated barrier stabilization. Furthermore, the relatively small effect in our experiments might be attributed to the

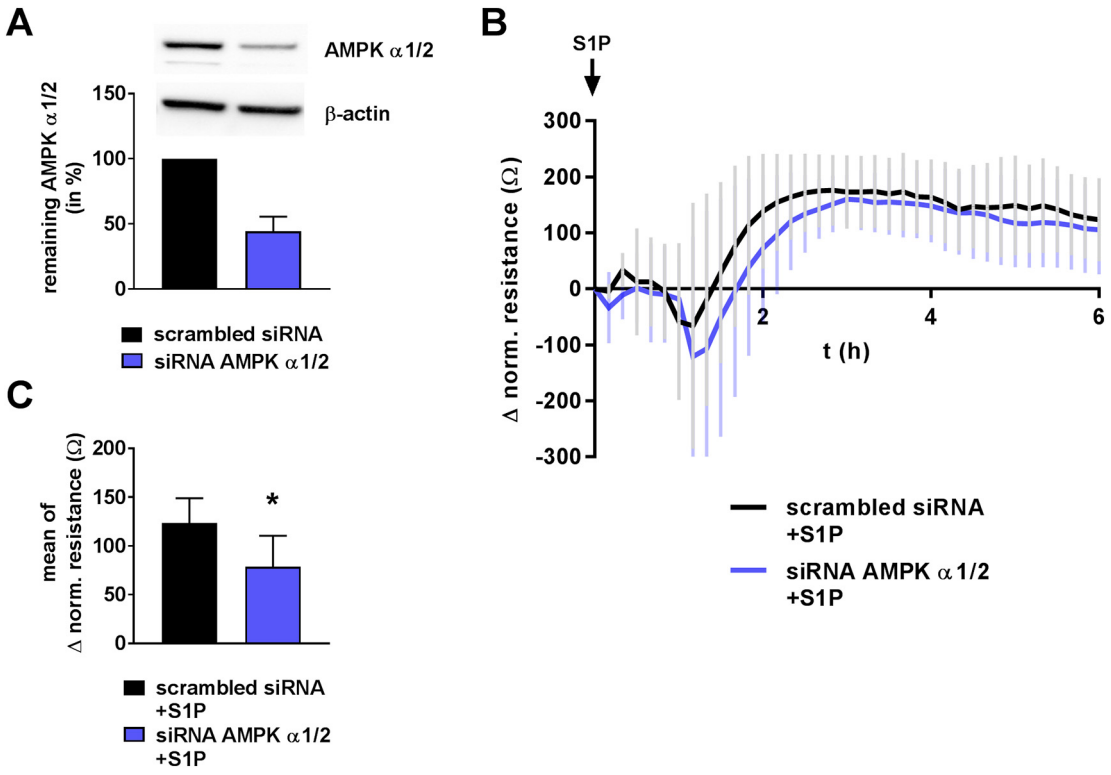

Fig. 3. AMPK partially mediates barrier-enhancing effects of S1P in HMEC-1. (A) Representative Western blots of AMPK α1/2 and β-actin loading control and quantification data (mean + SD, n = 3). (B) ECIS measurement of HMEC-1 reversely transfected with either scrambled siRNA or siRNA against AMPK α1/2 and stimulated with 1 μM S1P. Data are expressed as mean ± SD of 8–9 single measurements in 3 independent experiments. (C) S1P-induced changes in normalized mean resistance (relative to 10 min before S1P stimulation) of AMPK-deficient HMEC-1 compared to HMEC-1 treated with scrambled siRNA. Data are expressed as mean + SD, *p < 0.05 (Mann-Whitney-*U* test).

experimental setup, in which the electrodes of the ECIS™ array are covered by only approximately 500 cells. Thus, the percentage of AMPK knockdown might vary between the single experiments. Levine et al. demonstrated that AMPK phosphorylation by S1P modulates Rac1 signalling, indicating direct effects of S1P-phosphorylated AMPK on the cytoskeleton [25]. Tight junction molecules are known to regulate endothelial permeability and S1P was shown to contribute to the formation of tight junctions *via* Akt- and Rac-signalling [44]. Another well-known mediator of endothelial permeability, endothelial nitric oxide synthase (eNOS) [45], was shown to be regulated by S1P [46] and AMPK [47] resembling a potential link between the two, especially since S1P-mediated phosphorylation of eNOS was demonstrated to depend on AMPK in bovine and murine aortic endothelial cells [25,26].

3.4. FTY720 does not prevent endothelial barrier breakdown in our setting

As the S1P-AMPK interrelation appears to play a barrier-enhancing role in HMEC-1 under basal conditions, we further assessed potential barrier-protective effects by activating the S1P signalling pathway under inflammatory conditions. S1P has a very short half-life, hence we tested FTY720 instead. As Dudek et al. reported that FTY720 enhances barrier function in pulmonary endothelial cells by an alternative pathway to S1P and the $S1P_1$ receptor [14], we also tested FTY720 in GENCs. Resistance of HMEC-1 and GENC layers was monitored 24 h after administration of LPS + Cyt and application of FTY720 or vehicle (Fig. 4).

In our experimental setup, we observed no significant changes in resistance in HMEC-1, compared with the vehicle control (Fig. 4A). In GENCs, no effects of FTY720 were observed compared with the vehicle control (Fig. 4B).

We observed neither positive nor negative effects of FTY720 on the disturbed endothelial barrier in HMEC-1 or GENCs under the chosen experimental conditions. While others have described an adverse effect of the S1P-analogue leading to increased permeability [48], this indicates that FTY720 in the used dosage does not affect the endothelial barrier negatively during inflammation. Contrariwise, *in vivo* studies have shown that FTY720 reduced fluid extravasation in a rat model of sepsis [19] and diminished lung microvascular permeability in LPS-treated mice [20]. While FTY720 might have protective potential against inflammatory barrier disruption in the kidney, as demonstrated in a rat model of chronic kidney dysfunction [49], our findings in GENCs are in line with our previous observation that FTY720 did not significantly improve kidney function in septic mice [11]. Additionally, organ specificity of FTY720-mediated barrier protection may account for our results: endothelial cells derived from brain microcapillaries showed protective effects of FTY720 against inflammatory barrier breakdown [15] and we observed beneficial effects of FTY720 on the cardiac function of septic mice while kidney function was not improved [11]. Organ specificity could be mediated by differential expression of sphingosine kinases needed for FTY720 activation [50] or varying expression patterns of S1P receptor subtypes between tissues [51]. Furthermore, the timing of FTY720 administration and the dosage as well as the degree of the pro-inflammatory challenge may influence potential effects. This needs to be further investigated.

3.5. Conclusion

We established a reproducible and transferable *in vitro* model of inflammatory barrier breakdown that allows testing of interventional strategies. Our model revealed that the response of the endothelium to inflammatory stimuli highly depends on the origin of the endothelial cells. We furthermore demonstrated AMPK phosphorylation by S1P in cells of the microvascular but not in the glomerular endothelium and, for the first time, provided evidence for the functional role of the S1P/

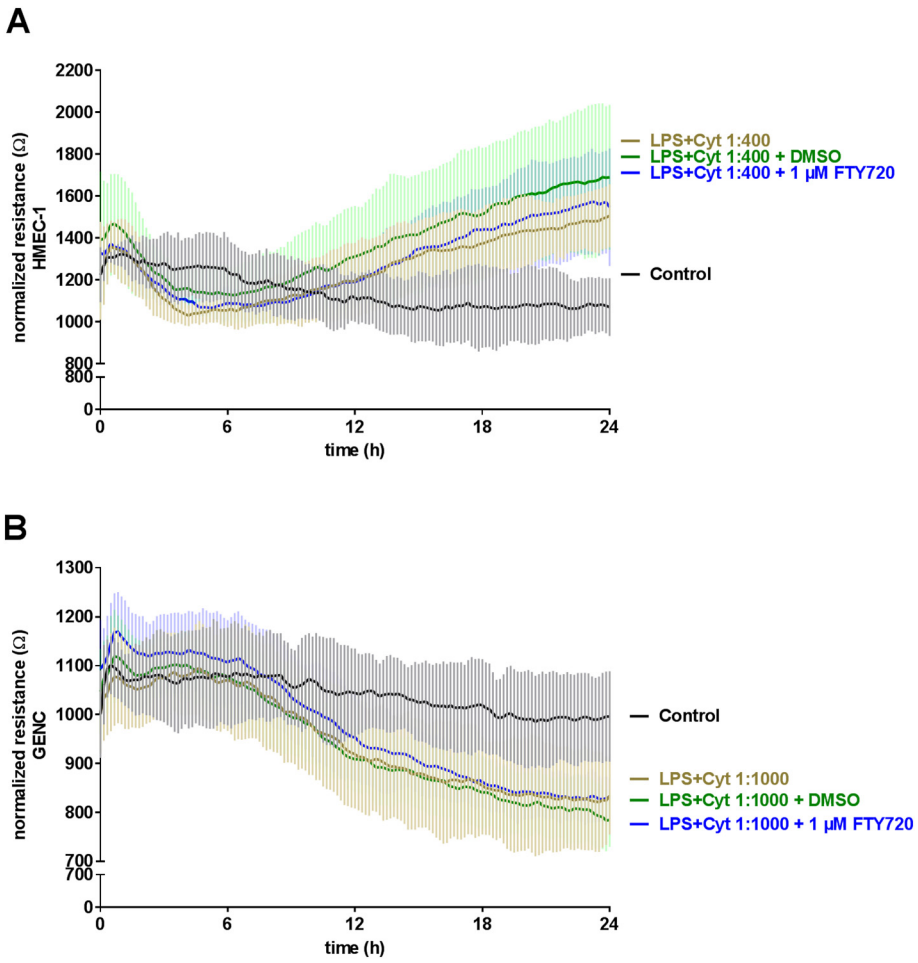

Fig. 4. Effects of FTY720 on endothelial barrier breakdown induced by an inflammatory stimulus in HMEC-1 and GENCs. ECIS measurement of endothelial barrier function in (A) HMEC-1 (n = 3) and (B) GENC (n = 4) cells co-stimulated at t = 0 h with inflammatory stimulus in the respective concentrations (LPS + Cyt; LPS, TNF-α, IL-1ß, IFN-γ, and IL–6) and 1 µM FTY720 or vehicle (DMSO). (A, B) Data are expressed as mean ± SD, n = 3–4 measurements, ns *vs.* LPS + Cyt + DMSO (two-way ANOVA with Holm-Sidak *post hoc*).

AMPK axis for barrier stabilization. Therefore, cell-type specific differences in the S1P-AMPK axis should be taken into account when testing interventional strategies to prevent barrier breakdown under inflammatory conditions.

Transparency document

The Transparency document associated with this article can be found, in online version.

Acknowledgements

This work was supported by the Federal Ministry of Education and Research, Germany (BMBF; ZIK Septomics Research Centre, Translational Septomics, award no. 03Z22JN12 to SMC and Center for Sepsis Control and Care, project TaSep, award no. 01EO1502 to SMC) and the Swiss National Science Foundation, Switzerland (310030_175561/1 to AH). KRF is a recipient of a scholarship by the "Interdisziplinäres Zentrum für Klinische Forschung" Jena. We would like to thank Michael P. Madaio for the kind permission to use GENCs. We thank Dr. Charles Neu for proofreading the manuscript prior to publication.

Authorship

SMC designed the study. SD and KRF performed and analysed experiments. SMC, SD, KRF, and AH wrote the manuscript. All authors carefully reviewed and approved the manuscript.

The authors declare no conflict of interest.

Appendix A. Supplementary data

Supplementary data to this article can be found online at https://doi.org/10.1016/j.bbadis.2018.12.022.

References

[1] D. De Backer, J. Creteur, J.C. Preiser, M.J. Dubois, J.L. Vincent, Microvascular blood flow is altered in patients with sepsis, Am. J. Respir. Crit. Care Med. 166 (2002) 98–104.
[2] Y. Sakr, M.J. Dubois, D. De Backer, J. Creteur, J.L. Vincent, Persistent microcirculatory alterations are associated with organ failure and death in patients with septic shock, Crit. Care Med. 32 (2004) 1825–1831.
[3] C. Ince, P.R. Mayeux, T. Nguyen, H. Gomez, J.A. Kellum, G.A. Ospina-Tascon, G. Hernandez, P. Murray, D. De Backer, A.X. Workgroup, The endothelium in sepsis, Shock 45 (2016) 259–270.
[4] S.M. Opal, T. van der Poll, Endothelial barrier dysfunction in septic shock, J. Intern. Med. 277 (2015) 277–293.
[5] M. Ksiazek, M. Chacinska, A. Chabowski, M. Baranowski, Sources, metabolism, and regulation of circulating sphingosine-1-phosphate, J. Lipid Res. 56 (2015) 1271–1281.
[6] J.G. Garcia, F. Liu, A.D. Verin, A. Birukova, M.A. Dechert, W.T. Gerthoffer, J.R. Bamberg, D. English, Sphingosine 1-phosphate promotes endothelial cell barrier integrity by Edg-dependent cytoskeletal rearrangement, J. Clin. Invest. 108 (2001) 689–701.
[7] X. Sun, Y. Shikata, L. Wang, K. Ohmori, N. Watanabe, J. Wada, K. Shikata,

K.G. Birukov, H. Makino, J.R. Jacobson, S.M. Dudek, J.G. Garcia, Enhanced interaction between focal adhesion and adherens junction proteins: involvement in sphingosine 1-phosphate-induced endothelial barrier enhancement, Microvasc. Res. 77 (2009) 304–313.
[8] X.E. Zhang, S.P. Adderley, J.W. Breslin, Activation of RhoA, but not Rac1, mediates early stages of S1P-induced endothelial barrier enhancement, PLoS One 11 (2016) e0155490.
[9] E. Camerer, J.B. Regard, I. Cornelissen, Y. Srinivasan, D.N. Duong, D. Palmer, T.H. Pham, J.S. Wong, R. Pappu, S.R. Coughlin, Sphingosine-1-phosphate in the plasma compartment regulates basal and inflammation-induced vascular leak in mice, J. Clin. Invest. 119 (2009) 1871–1879.
[10] M. Tauseef, V. Kini, N. Knezevic, M. Brannan, R. Ramchandaran, H. Fyrst, J. Saba, S.M. Vogel, A.B. Malik, D. Mehta, Activation of sphingosine kinase-1 reverses the increase in lung vascular permeability through sphingosine-1-phosphate receptor signaling in endothelial cells, Circ. Res. 103 (2008) 1164–1172.
[11] S.M. Coldewey, E. Benetti, M. Collino, J. Pfeilschifter, C. Sponholz, M. Bauer, A. Huwiler, C. Thiemermann, Elevation of serum sphingosine-1-phosphate attenuates impaired cardiac function in experimental sepsis, Sci. Rep. 6 (2016) 27594.
[12] C. Frej, A. Linder, K.E. Happonen, F.B. Taylor, F. Lupu, B. Dahlback, Sphingosine 1-phosphate and its carrier apolipoprotein M in human sepsis and in Escherichia coli sepsis in baboons, J. Cell. Mol. Med. 20 (2016) 1170–1181.
[13] M.S. Winkler, A. Nierhaus, M. Holzmann, E. Mudersbach, A. Bauer, L. Robbe, C. Zahrte, M. Geffken, S. Peine, E. Schwedhelm, G. Daum, S. Kluge, C. Zoellner, Decreased serum concentrations of sphingosine-1-phosphate in sepsis, Crit. Care 19 (2015) 372.
[14] S.M. Dudek, S.M. Camp, E.T. Chiang, P.A. Singleton, P.V. Usatyuk, Y. Zhao, V. Natarajan, J.G. Garcia, Pulmonary endothelial cell barrier enhancement by FTY720 does not require the S1P1 receptor, Cell. Signal. 19 (2007) 1754–1764.
[15] F. Imeri, S. Schwalm, R. Lyck, A. Zivkovic, H. Stark, B. Engelhardt, J. Pfeilschifter, A. Huwiler, Sphingosine kinase 2 deficient mice exhibit reduced experimental autoimmune encephalomyelitis: resistance to FTY720 but not ST-968 treatments, Neuropharmacology 105 (2016) 341–350.
[16] L. Wang, E.T. Chiang, J.T. Simmons, J.G. Garcia, S.M. Dudek, FTY720-induced human pulmonary endothelial barrier enhancement is mediated by c-Abl, Eur. Respir. J. 38 (2011) 78–88.
[17] T. Sanchez, T. Estrada-Hernandez, J.H. Paik, M.T. Wu, K. Venkataraman, V. Brinkmann, K. Claffey, T. Hla, Phosphorylation and action of the immunomodulator FTY720 inhibits vascular endothelial cell growth factor-induced vascular permeability, J. Biol. Chem. 278 (2003) 47281–47290.
[18] F. Imeri, D. Fallegger, A. Zivkovic, S. Schwalm, G. Enzmann, K. Blankenbach, D. Meyer zu Heringdorf, T. Homann, B. Kleuser, J. Pfeilschifter, B. Engelhardt, H. Stark, A. Huwiler, Novel oxazolo-oxazole derivatives of FTY720 reduce endothelial cell permeability, immune cell chemotaxis and symptoms of experimental autoimmune encephalomyelitis in mice, Neuropharmacology 85 (2014) 314–327.
[19] C. Lundblad, H. Axelberg, P.O. Grande, Treatment with the sphingosine-1-phosphate analogue FTY 720 reduces loss of plasma volume during experimental sepsis in the rat, Acta Anaesthesiol. Scand. 57 (2013) 713–718.
[20] X. Peng, P.M. Hassoun, S. Sammani, B.J. McVerry, M.J. Burne, H. Rabb, D. Pearse, R.M. Tuder, J.G. Garcia, Protective effects of sphingosine 1-phosphate in murine endotoxin-induced inflammatory lung injury, Am. J. Respir. Crit. Care Med. 169 (2004) 1245–1251.
[21] N.A. Shirwany, M.H. Zou, AMPK: a cellular metabolic and redox sensor. A minireview, Front. Biosci. (Landmark Ed.) 19 (2014) 447–474.
[22] D.A. Escobar, A.M. Botero-Quintero, B.C. Kautza, J. Luciano, P. Loughran, S. Darwiche, M.R. Rosengart, B.S. Zuckerbraun, H. Gomez, Adenosine monophosphate-activated protein kinase activation protects against sepsis-induced organ injury and inflammation, J. Surg. Res. 194 (2015) 262–272.
[23] J. Xing, Q. Wang, K. Coughlan, B. Viollet, C. Moriasi, M.H. Zou, Inhibition of AMP-activated protein kinase accentuates lipopolysaccharide-induced lung endothelial barrier dysfunction and lung injury in vivo, Am. J. Pathol. 182 (2013) 1021–1030.
[24] Z. Zhao, J. Hu, X. Gao, H. Liang, Z. Liu, Activation of AMPK attenuates lipopolysaccharide-impaired integrity and function of blood-brain barrier in human brain microvascular endothelial cells, Exp. Mol. Pathol. 97 (2014) 386–392.
[25] Y.C. Levine, G.K. Li, T. Michel, Agonist-modulated regulation of AMP-activated protein kinase (AMPK) in endothelial cells. Evidence for an AMPK → Rac1 → Akt → endothelial nitric-oxide synthase pathway, J. Biol. Chem. 282 (2007) 20351–20364.
[26] T. Kimura, H. Tomura, K. Sato, M. Ito, I. Matsuoka, D.S. Im, A. Kuwabara, C. Mogi, H. Itoh, H. Kurose, M. Murakami, F. Okajima, Mechanism and role of high density lipoprotein-induced activation of AMP-activated protein kinase in endothelial cells, J. Biol. Chem. 285 (2010) 4387–4397.
[27] F.A. Malik, A. Meissner, I. Semenkov, S. Molinski, S. Pasyk, S. Ahmadi, H.H. Bui, C.E. Bear, D. Lidington, S.S. Bolz, Sphingosine-1-phosphate is a novel regulator of cystic fibrosis transmembrane conductance regulator (CFTR) activity, PLoS One 10 (2015) e0130313.
[28] V. Spindler, N. Schlegel, J. Waschke, Role of GTPases in control of microvascular permeability, Cardiovasc. Res. 87 (2010) 243–253.
[29] W.C. Aird, Endothelial cell heterogeneity, Cold Spring Harb. Perspect. Med. 2 (2012) a006429.
[30] S. Uchino, J.A. Kellum, R. Bellomo, G.S. Doig, H. Morimatsu, S. Morgera, M. Schetz, I. Tan, C. Bouman, E. Macedo, N. Gibney, A. Tolwani, C. Ronco, I. Beginning, Ending supportive therapy for the kidney, acute renal failure in critically ill patients: a multinational, multicenter study, JAMA 294 (2005) 813–818.
[31] C. Xu, A. Chang, B.K. Hack, M.T. Eadon, S.L. Alper, P.N. Cunningham, TNF-mediated damage to glomerular endothelium is an important determinant of acute kidney injury in sepsis, Kidney Int. 85 (2014) 72–81.
[32] N. Akis, M.P. Madaio, Isolation, culture, and characterization of endothelial cells from mouse glomeruli, Kidney Int. 65 (2004) 2223–2227.
[33] I. Giaever, C.R. Keese, Micromotion of mammalian cells measured electrically, Proc. Natl. Acad. Sci. U. S. A. 88 (1991) 7896–7900.
[34] J. Ziauddin, D.M. Sabatini, Microarrays of cells expressing defined cDNAs, Nature 411 (2001) 107–110.
[35] Q. Huang, T. Whitington, P. Gao, J.F. Lindberg, Y. Yang, J. Sun, M.R. Vaisanen, R. Szulkin, M. Annala, J. Yan, L.A. Egevad, K. Zhang, R. Lin, A. Jolma, M. Nykter, A. Manninen, F. Wiklund, M.H. Vaarala, T. Visakorpi, J. Xu, J. Taipale, G.H. Wei, A prostate cancer susceptibility allele at 6q22 increases RFX6 expression by modulating HOXB13 chromatin binding, Nat. Genet. 46 (2014) 126–135.
[36] D.M. Shasby, S.S. Shasby, J.M. Sullivan, M.J. Peach, Role of endothelial cell cytoskeleton in control of endothelial permeability, Circ. Res. 51 (1982) 657–661.
[37] D. Chakravortty, N. Koide, Y. Kato, T. Sugiyama, M. Kawai, M. Fukada, T. Yoshida, T. Yokochi, Cytoskeletal alterations in lipopolysaccharide-induced bovine vascular endothelial cell injury and its prevention by sodium arsenite, Clin. Diagn. Lab. Immunol. 7 (2000) 218–225.
[38] S.E. Goldblum, X. Ding, T.W. Brann, J. Campbell-Washington, Bacterial lipopolysaccharide induces actin reorganization, intercellular gap formation, and endothelial barrier dysfunction in pulmonary vascular endothelial cells: concurrent F-actin depolymerization and new actin synthesis, J. Cell. Physiol. 157 (1993) 13–23.
[39] P. He, M.J. Philbrick, X. An, J. Wu, A.F. Messmer-Blust, J. Li, Endothelial differentiation gene-1, a new downstream gene is involved in RTEF-1 induced angiogenesis in endothelial cells, PLoS One 9 (2014) e88143.
[40] S. Wang, Z. Zhang, X. Lin, D.S. Xu, Y. Feng, K. Ding, A polysaccharide, MDG-1, induces S1P1 and bFGF expression and augments survival and angiogenesis in the ischemic heart, Glycobiology 20 (2010) 473–484.
[41] T. Sanchez, A. Skoura, M.T. Wu, B. Casserly, E.O. Harrington, T. Hla, Induction of vascular permeability by the sphingosine-1-phosphate receptor-2 (S1P2R) and its downstream effectors ROCK and PTEN, Arterioscler. Thromb. Vasc. Biol. 27 (2007) 1312–1318.
[42] J.F. Lee, S. Gordon, R. Estrada, L. Wang, D.L. Siow, B.W. Wattenberg, D. Lominadze, M.J. Lee, Balance of S1P1 and S1P2 signaling regulates peripheral microvascular permeability in rat cremaster muscle vasculature, Am. J. Physiol. Heart Circ. Physiol. 296 (2009) H33–H42.
[43] J. Creighton, M. Jian, S. Sayner, M. Alexeyev, P.A. Insel, Adenosine monophosphate-activated kinase alpha1 promotes endothelial barrier repair, FASEB J. 25 (2011) 3356–3365.
[44] J.F. Lee, Q. Zeng, H. Ozaki, L. Wang, A.R. Hand, T. Hla, E. Wang, M.J. Lee, Dual roles of tight junction-associated protein, zonula occludens-1, in sphingosine 1-phosphate-mediated endothelial chemotaxis and barrier integrity, J. Biol. Chem. 281 (2006) 29190–29200.
[45] A. Di Lorenzo, M.I. Lin, T. Murata, S. Landskroner-Eiger, M. Schleicher, M. Kothiya, Y. Iwakiri, J. Yu, P.L. Huang, W.C. Sessa, eNOS-derived nitric oxide regulates endothelial barrier function through VE-cadherin and Rho GTPases, J. Cell Sci. 126 (2013) 5541–5552.
[46] J. Igarashi, S.G. Bernier, T. Michel, Sphingosine 1-phosphate and activation of endothelial nitric-oxide synthase. Differential regulation of Akt and MAP kinase pathways by EDG and bradykinin receptors in vascular endothelial cells, J. Biol. Chem. 276 (2001) 12420–12426.
[47] Z.P. Chen, K.I. Mitchelhill, B.J. Michell, D. Stapleton, I. Rodriguez-Crespo, L.A. Witters, D.A. Power, P.R. Ortiz de Montellano, B.E. Kemp, AMP-activated protein kinase phosphorylation of endothelial NO synthase, FEBS Lett. 443 (1999) 285–289.
[48] B.S. Shea, S.F. Brooks, B.A. Fontaine, J. Chun, A.D. Luster, A.M. Tager, Prolonged exposure to sphingosine 1-phosphate receptor-1 agonists exacerbates vascular leak, fibrosis, and mortality after lung injury, Am. J. Respir. Cell Mol. Biol. 43 (2010) 662–673.
[49] H. Ni, J. Chen, M. Pan, M. Zhang, J. Zhang, P. Chen, B. Liu, FTY720 prevents progression of renal fibrosis by inhibiting renal microvasculature endothelial dysfunction in a rat model of chronic kidney disease, J. Mol. Histol. 44 (2013) 693–703.
[50] A. Billich, F. Bornancin, P. Devay, D. Mechtcheriakova, N. Urtz, T. Baumruker, Phosphorylation of the immunomodulatory drug FTY720 by sphingosine kinases, J. Biol. Chem. 278 (2003) 47408–47415.
[51] T. Sanchez, T. Hla, Structural and functional characteristics of S1P receptors, J. Cell. Biochem. 92 (2004) 913–922.